

# Modeling of the Conveying of Solid Polymer in the Feeding Zone of Intermeshing Co-rotating Twin Screw Extruders

C. CARROT, J. GUILLET, J. F. MAY and J. P. PUAUX

*Laboratoire de Rhéologie des Matières plastiques  
Faculté de Sciences et Techniques  
Université Jean Monnet  
42023 Saint-Etienne Cedex 02. France*

In this paper, a model for the conveying of solid polymer in the feeding zone of intermeshing co-rotating twin screw extruders is proposed. The theoretical model uses an approach that is similar to that commonly used in single screw extruders; however, it takes into account the particular geometry of the screw channel, the partially filled channel, and the special configuration of the two self-wiping screws. The model thus considers two conveying mechanisms: the first one in the channel, which is analyzed in terms of polymer-metal friction, and the second one, which is mainly an axial transport in the intermeshing zone. The theoretical predictions of the model are compared with the experimental results obtained on a laboratory extruder with a polymer in powder form, and satisfactory agreement is observed. The model enables the prediction of the evolution of the filling of the screws towards the geometry and the operating conditions. This is an important key to analyzing the thermal aspects in this zone, which can lead to a prediction of the melting capacity of the extruder. Indeed, the filling of the feeding zone defines the heat transport that occurs between the hot barrel and the solid polymer.

## INTRODUCTION

The modeling of the conveying of molten polymer in the intermeshing co-rotating twin screw extruders has been widely discussed in the literature. Finite element analysis (1-4) and analytical models (5, 6) have been proposed and provide satisfactory results to predict the pumping characteristics of the extruder either in the screw zones or in the kneading discs (7, 8).

However, the feeding and melting zones, where the polymer is in the solid state or a combination of molten polymer and solid, have been less well studied. The knowledge on this important subject is rather qualitative, as for example the relative insensitivity of this type of extruder to the friction coefficient between polymer and metal in the feeding zone, which enables the extrusion for liquids or sticking materials (9).

Yet there is a great interest in this type of modeling. First of all, it allows the prediction of limiting factors for the throughput of the extruder. Moreover, the modeling of the entire process needs a previous investigation of the thermal history of the polymer that defines the minimal length needed for the transition to a molten state to occur. The optimization of a

screw profile for a given application can only be achieved by a deeper knowledge of the melting capacity of the screws, and thus by a good understanding of the conveying mechanisms in the feeding zone.

The former point needs further comment. In fact, the operating conditions in this type of extruder are quite different from that encountered in a single screw extruder. In standard conditions, there is only a partial filling of the screws, and it depends on both the geometry and the operating conditions as the throughput or the rotational speed. So, thermal exchanges between the heat source, the barrel, and the polymer can be greatly modified by a change in the operating parameters, and the melting capacity of the machine is altered in an important manner.

The aim of the present work is to propose a theoretical model for the conveying of the solid material in the feeding zone and thus to enable the calculation of the filling of the screw in various conditions.

## THEORETICAL MODEL

### Screw Geometry

The calculation of screw geometry is the basic analysis necessary for the understanding of the phenom-

ena involved in the conveying of material either in the solid or in the molten state. Such a description has been performed by Booy (5, 10). According to this work, the geometrical description of the screw in a self-wiping co-rotating twin screw extruder can be completely performed by mean of a limited number of parameters, which are: the outer diameter of the screws or the barrel diameter  $D$ , the centerline distance  $C_L$ , the number of flight starts  $m$ , and the pitch  $T$ . If these parameters are known, other important parameters can be calculated, such as:

$$\theta = \text{screw angle at the barrel diameter} = \tan^{-1} \left( \frac{T}{\pi D} \right) \quad (1)$$

$$\rho_c = \frac{2C_L}{D} \quad (2)$$

$\psi$  = angle of the intermeshing zone

$$= \cos^{-1} \left( \frac{\rho_c}{2} \right) = \cos^{-1} \left( \frac{C_L}{D} \right) \quad (3)$$

The various geometrical parameters can be seen on Figs. 1a and 1b. Moreover, the self-wiping condition can be satisfied only in the screw arrangement shown in Fig. 1b. Thus, for a screw with two flight starts, the various parameters are fixed, and there is a single configuration for the screw that enables the calculation of a single channel geometry. In Fig. 1b, a cross section of the barrel normal to the screw axis is sketched. The cross section of a screw can be described as a "quasi-ellipsoidal" surface, which has the following characteristics:

- on an angle  $\alpha$  on the great axis of the "ellipsoid," the radius is  $\frac{D}{2}$ ;
- on the same angle  $\alpha$  on the small axis of the "ellipsoid," the radius is  $\frac{2C_L - D}{2}$ ;
- on an angle  $2\psi$  between the two previous zones, the radius is  $C_L$ .

The maximum depth of the channel can then be calculated:

$$h_0 = D - C_L \quad (4)$$

and the flight angle at the barrel diameter is given by:

$$\alpha = \frac{\pi}{m} - 2 \cos^{-1} \left( \frac{\rho_c}{2} \right) \quad (5)$$

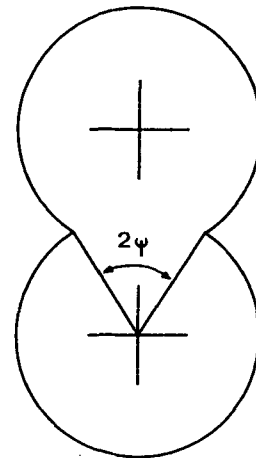
### Channel Geometry

Figure 1b enables the calculation of the channel geometry as a function of the angle  $\lambda$ , and thus:

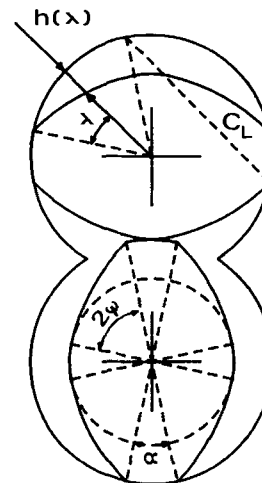
$$h(\lambda) = \frac{D}{2} \left\{ 1 + \cos \lambda - \sqrt{\rho_c^2 - \sin^2 \lambda} \right\} \quad (6)$$

for  $0 < \lambda < 2\psi$

Unrolling the barrel and the screw, the channel geometry in a plane normal to the channel axis can be described as shown in Fig. 2. In the coordinate system based on  $x$ , the depth of the channel at



(a)



(b)

Fig. 1. Geometrical description of the twin screw arrangement (cross section normal to the screw axis for a two-flighted screw).

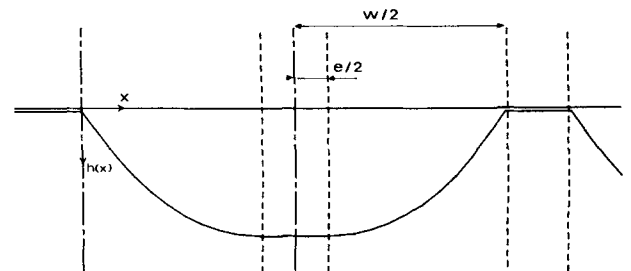


Fig. 2. Geometrical description of the screw channel (cross section normal to the channel axis).

various positions is given by:

$$h(x) = \frac{D}{2} \left\{ 1 + \cos \Lambda - \sqrt{\rho_c^2 - \sin^2 \Lambda} \right\}$$

with

$$\Lambda = \frac{2\pi \left( x - \frac{w-e}{2} \right)}{T \cos \theta} \quad \text{for } 0 < x < \frac{w-e}{2} \quad (7a)$$

$$\Lambda = \frac{2\pi \left( x - \frac{w+e}{2} \right)}{T \cos \theta} \quad \text{for } \frac{w+e}{2} < x < w \quad (7b)$$

$$h(x) = h_0 = D - C_L \quad \text{for } \frac{w-e}{2} < x < \frac{w+e}{2} \quad (7c)$$

$$h(x) = 0 \quad \text{for } w < x < w + \frac{e}{2} \quad (7d)$$

where

$$e = \text{flight width normal to the channel axis} \\ = \frac{T \alpha \cos \theta}{2\pi} \quad (8)$$

$$w = \text{channel width normal to the channel axis} \\ = \frac{T}{m} \left( 1 - \frac{\alpha m}{2\pi} \right) \cos \theta \quad (9)$$

### Modeling of the Entire Twin Screw Arrangement

In the proposed model, the two screws are described by  $2m-1$  parallel channels, each with the previous geometry. The intermeshing zone is considered separately.

In the channels, material conveying is mainly due to the friction of solid polymer with both the barrel and the screw. In the intermeshing zone, the solid polymer is transported in the axial direction by a distance of the pitch for every revolution of the screw shaft, whatever the operating conditions are.

### Material Conveying in the intermeshing Zone

As stated, in this zone the material is transported by a distance equal to the pitch for every resolution of the screw. So the volume throughput in this zone can be expressed by

$$Q_E = A_E n T \quad (10)$$

where  $n$  is the rotational speed of the screws, and  $A_E$  is the intermeshing zone area.

For a two-flighted screw and according to the various areas described in Fig. 3, which are all estimated in the plane normal to the screw axis:

$$A_E = A_L - (2m-1) A_C = A_L - 3 A_C \\ = (A_F - 2 A_D) - \frac{3}{2} (A_U - A_D) \quad (11)$$

where  $A_L$  is the free area between the barrel and the screws,  $A_C$  is the channel area,  $A_F$  is barrel area,  $A_D$  is the screw area, and  $A_U$  is the area of an half of a barrel.

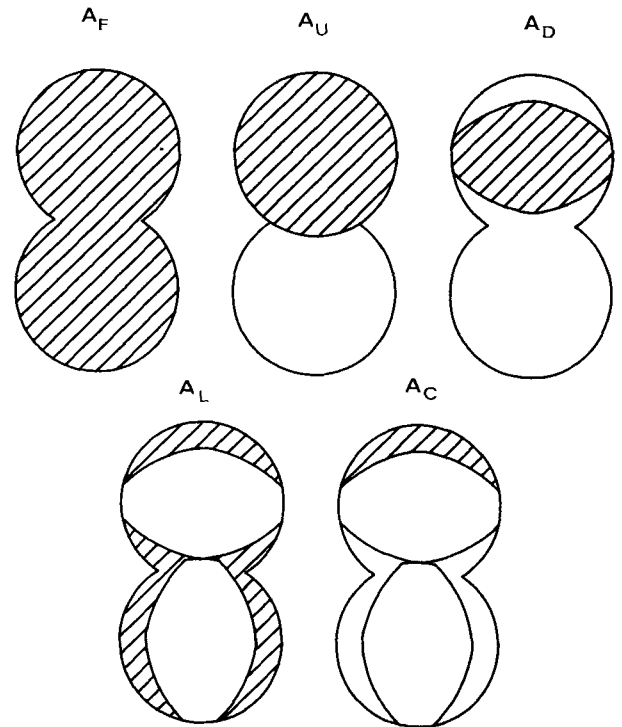


Fig. 3. Various areas used in calculations (cross section normal to the screw axis).

Geometrical calculations of the various areas lead to:

$$A_U = \pi \frac{D^2}{4} \quad (12)$$

$$A_F = \{2(\pi - \psi) + \rho_c \sin \psi\} \frac{D^2}{4} \quad (13)$$

$$A_D = \{\alpha[\rho_c^2 - 2\rho_c + 2] + 2\psi\rho_c^2 - 2\rho_c \sin \psi\} \frac{D^2}{4} \quad (14)$$

$$A_L = \{5\rho_c \sin \psi + 2(\pi - \psi) - 2\alpha[\rho_c^2 - 2\rho_c + 2] - 4\psi\rho_c^2\} \frac{D^2}{4} \quad (15)$$

$$A_C = \left\{ \frac{\pi}{2} - \psi\rho_c^2 + \rho_c \sin \psi - \frac{\alpha}{2}[\rho_c^2 - 2\rho_c + 2] \right\} \frac{D^2}{4} \quad (16)$$

$$A_E = \left\{ \frac{\alpha}{2}[2\rho_c - \rho_c^2] - \psi\rho_c^2 + 2\rho_c \sin \psi \right\} \frac{D^2}{4} \quad (17)$$

Finally, the maximum throughput in the intermeshing zone can be rewritten as:

$$Q_E = n T \frac{D^2}{4} \rho_c \left\{ \frac{\alpha}{2}[2 - \rho_c] - \psi\rho_c + 2 \sin \psi \right\} \quad (18)$$

This throughput depends only on the geometrical characteristics of the machine and on the rotational speed.

### Material Conveying in the Channels

In the channel of the screw, the calculation of the solid polymer conveying is performed through the use of an approach that is nearly that of Tadmor in a single screw extruder (11). In the channel, the solid in contact with both the screw and the barrel is conveyed under the influence of the friction forces and of the screw rotation. The direction of the friction forces, known as the "Coulomb forces," is opposed to that of the relative speed of the solid versus the support, as described in Fig. 4, and their intensity is given by:

$$F = pSf \quad (19)$$

where  $p$  is the contact pressure,  $S$  is the area of the contact surface, and  $f$  is the friction coefficient.

Thus in the channel, a solid element  $V$ , which partially fills the channel, is transported at the speed  $u$ . This speed is determined by the angle  $\Phi$  between the friction force on the solid due to the barrel and the barrel speed, as shown in Fig. 5.

Letting  $A(x_b)$  be the area of the channel occupied by the solid material, the throughput in a channel is then given by:

$$Q'_C = \frac{A(x_b)}{\sin \theta_m} = u \sin \theta \quad (20)$$

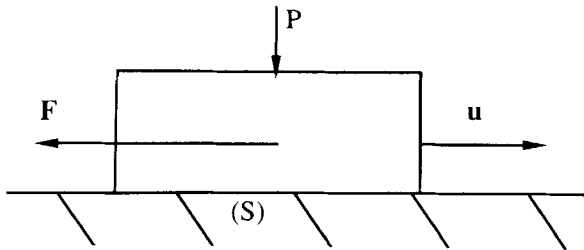


Fig. 4. Schematic description of the friction forces for a solid volume moving on a plane.

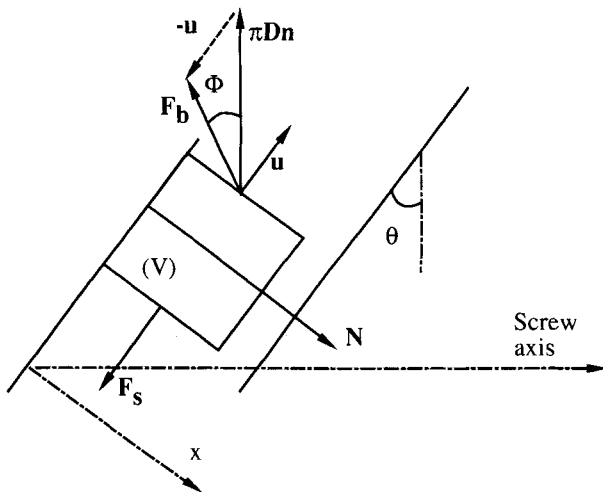


Fig. 5. Schematic description of the various forces acting on a solid element in the channel.

where  $x_b$  is the width of the channel that is filled with material, measured at the barrel diameter, and  $\theta_m$  is the average value of the angle  $\theta$ .

It is necessary to define  $\theta_m$ , which can be significantly different from the value of  $\theta$  at the barrel diameter because of the large channel depth encountered in this type of machine.  $\theta_m$  is given by:

$$\begin{aligned} \theta_m &= \operatorname{tg}^{-1} \left( \frac{T}{\pi D_m} \right) = \operatorname{tg}^{-1} \left( \frac{T}{\pi (D - h_0)} \right) \\ &= \operatorname{tg}^{-1} \left( \frac{T}{\pi C_L} \right) \end{aligned} \quad (21)$$

where

$$D_m \text{ is the average diameter} = D - h_0 = C_L \quad (22)$$

$u \sin \theta$  can be calculated by the use of the relation:

$$\operatorname{tg} \Phi = \frac{u \sin \theta}{\pi D n - u \cos \Phi} \quad (23)$$

and finally, combining Eqs 22 and 23:

$$u \sin \theta = \pi D n \frac{\operatorname{tg} \Phi \operatorname{tg} \theta}{\operatorname{tg} \Phi + \operatorname{tg} \theta} \quad (24)$$

Determination of angle  $\Phi$  can be performed through a force and momentum balance on the solid element  $V$ , as indicated in Fig. 5. In a first approximation, the cross section of the channel is considered to be nearly rectangular. Its ceiling is the barrel and its floor is the screw root.

Three main forces act on the material:

- The friction of solid with the barrel, which is applied at the barrel diameter  $D$ :

$$F_b = f_b x_b p z_b \quad (25)$$

where  $f_b$  is the friction coefficient of the material with the barrel,  $z_b$  is the length of the volume element  $V$  at the barrel diameter,  $x_b$  is the dimension of the volume element  $V$ , in a direction normal to the screw flight at the barrel diameter, and  $p$  is the contact pressure.

- The friction of solid with the screw, applied at the screw root diameter  $D_s = 2C_L - D$ :

$$F_s = f_s x_s p z_s \quad (26)$$

where  $f_s$  is the friction coefficient of the material with the screw, and  $z_s$  is the length of the volume element  $V$  at the screw diameter.

$$z_s = z_b \frac{\sin \theta}{\sin \theta_s} \quad (27)$$

and

$$\theta_s = \operatorname{tg}^{-1} \left( \frac{T}{\pi D_s} \right) = \operatorname{tg}^{-1} \left( \frac{T}{\pi (2C_L - D)} \right) \quad (28)$$

$x_s$  is the dimension of the volume element  $V$ , in a

direction normal to the screw flight at the screw root.

- An additional force  $\mathbf{N}$  including the flight pushing action.  $\mathbf{N}$  is normal to the flight and can be considered as applied at the average diameter  $D_m = C_L$ .

The force and momentum balances can be written as:

$$F_b \sin \Phi + F_s \sin \theta_s = N \cos \theta_m \quad (29)$$

and

$$F_s \cos \theta_s D_s + N \sin \theta_m D_m = F_b \cos \Phi D \quad (30)$$

Eliminating  $N$  between the previous equations leads to:

$$\begin{aligned} \cos \Phi &= \sin \Phi \tan \theta_m \frac{D_m}{D} + \frac{F_s}{F_b} \frac{D_m}{D} \frac{\sin \theta_m}{\cos \theta_m} \sin \theta_s \\ &+ \frac{F_s}{F_b} \frac{D_s}{D} \cos \theta_s \quad (31) \\ &= K \sin \Phi + M \end{aligned}$$

where

$$K = \tan \theta \quad (32)$$

and

$$M = \frac{x_s}{x_b} \frac{f_s}{f_b} \frac{\sin \theta \tan \theta}{(\sin \theta_s)^2} \quad (33)$$

At this point, the  $\frac{x_s}{x_b}$  ratio can be chosen to take into account the particular geometry of the channel. It is, in the most general case, a function of  $x_b$ . However, an average value of this ratio will be considered as a first approximation.

The previous equation, which can be solved only when  $M < 1$ , gives the following solution according to Agassant, *et al.* (12):

$$\sin \Phi = \frac{\sqrt{1 + K^2 - M^2} - KM}{1 + K^2} \quad (34)$$

and the channel throughput (Eq 20) is finally:

$$Q'_C = \frac{\pi D n}{\sin \theta_m} \frac{\tan \Phi \tan \theta}{\tan \Phi + \tan \theta} A(x_b) \quad (35)$$

where

$$A(x_b) = \int_0^{x_b} dA = \int_0^{x_b} h(x) dx \quad (36)$$

For the two screws together, with two flight starts, the total throughput of the channels is:

$$\begin{aligned} Q_C &= (2m - 1) Q'_C \\ &= 3 Q'_C \\ &= 3 \frac{\pi D n}{\sin \theta_m} \frac{\tan \Phi \tan \theta}{\tan \Phi + \tan \theta} \int_0^{x_b} h(x) dx \quad (37) \end{aligned}$$

## EXPERIMENTAL WORK

### Experimental Method of Verification

Direct verification of Eqs 18 and 37 is not possible. However, an indirect method can be used by measurements of the screw filling vs. the operating conditions. This simple measurement can be performed by weighing the mass of material in the screw as a function of the throughput of the extruder. In stable operating conditions (fixed geometry, given rotational speed, throughput imposed by a feeding device), the feeding is suddenly interrupted and the remaining mass of solid in the screw is then weighed until the screw is empty.

The theoretical volume of material in the intermeshing zone can be evaluated. If  $L$  is the screw length, it is given by:

$$V_E = A_E L \quad (38)$$

The volume throughput is then given by Eq 10. When the volume throughput  $Q$  is less than  $Q_E$ ,

$$Q = \kappa Q_E \quad \text{with } 0 < \kappa < 1 \quad (39)$$

The volume in the screw is

$$V = \kappa V_E \quad (40)$$

Thus, below the maximum throughput of this zone  $Q_E$ , a plot  $V$  vs.  $Q$  should yield a straight line with a slope of:

$$S_E = \frac{L}{nT} \quad (41)$$

As far as the throughput is greater than  $Q_E$ , material conveying takes place both in the intermeshing zone and in the channels of the screws. Material volume in the channels is given by:

$$V_C = 3 \frac{L}{\sin \theta_m} \int_0^{x_b} h(x) dx \quad (42)$$

and above  $Q_E$ , a plot of  $V$  vs.  $Q$  yields a straight line with a slope of:

$$S_C = \frac{L}{\pi D n} \frac{\tan \Phi + \tan \theta}{\tan \Phi \tan \theta} \quad (43)$$

Experimental investigations were performed on a modular intermeshing co-rotating twin screw extruder. The experimental work was carried out on three types of screw elements with different pitches (16, 25, and 33 mm). The geometrical parameters of the extruder and the various characteristic areas and volumes needed in the calculations are summarized in Table 1. Owing to the modular conception of the machine, a screw length of 275 mm between the feeding port and the exit was used. High density polyethylene in powder form was used as solid material. Various operating conditions (throughput and rotational speed) were tested. Tests at two different temperatures of the barrel (20 and 100°C) were performed in order to show a possible influence of the friction coefficients.

Figure 6 shows a typical plot of the mass of material in the screw vs. the mass throughput for screws

with a pitch equal to 25 mm and various rotational speeds. Whatever the screw geometry and the operating conditions are, the maximum mass in the screw was found to be nearly constant, as can be seen in Table 3. This is consistent with Eq 15, which states that the free area between the barrel and the screw, defining the maximum free volume in the extruder, does not depend on the pitch or on the operating conditions. Calculations of an average density of the conveyed material, with a theoretical free volume of 85.2 cm<sup>3</sup>, yields a typical value of 0.5.

### Reduced Plot $M = f(Q/n)$

According to Eqs 18 and 37, the proposed model should yield a single master curve when the mass in

**Table 1. Geometrical Parameters and Various Areas for the Screw Elements Considered in the Experimental Work.**

	Screw 1	Screw 2	Screw 3
$T$ (mm)	16	25	33
$D$ (mm)	25	25	25
$C_L$ (mm)	21	21	21
$h_0$ (mm)	4	4	4
$\psi$ (°)	32.86	32.86	32.86
$\rho_c$	1.68	1.68	1.68
$m$	2	2	2
$\alpha$ (°)	24.28	24.28	24.28
$\theta$ (°)	11.51	17.66	22.79
$e$ (mm)	1.06	1.61	2.05
$w$ (mm)	6.78	10.30	13.15
$A_L$ (mm <sup>2</sup> )	309.8	309.8	309.8
$A_C$ (mm <sup>2</sup> )	86.6	86.6	86.6
$A_E$ (mm <sup>2</sup> )	50.0	50.0	50.0
$V_L$ (cm <sup>3</sup> )	85.2	85.2	85.2
$V_C$ (cm <sup>3</sup> )	23.8	23.8	23.8
$V_E$ (cm <sup>3</sup> )	13.7	13.7	13.7
$\left(\frac{x_s}{x_b}\right)$	1.860	1.461	1.312

the screw ( $M$ ) is plotted vs. the ratio of the throughput to the rotational speed, named the reduced throughput ( $Q/n$ ). And indeed, as can be seen in Fig. 7, the experimental results are in agreement with this particular feature of the model. This representation was found to work for various pitches and barrel temperatures. The maximum reduced throughput of the extruder was found to increase with increasing pitch. A slight increase of it was also observed when the barrel temperature was raised from 20 to 100°C, as can be seen in Table 3. This seems to indicate that friction coefficients should have an influence on the conveying characteristic of the screws.

### Comparison Between Theory and Experiment in the Intermeshing Zone

As stated previously by the model, for low throughput  $Q < QE$ , when material conveying takes place in the intermeshing zone, the plot of the mass in the screw vs. the reduced throughput is a straight line. This is in agreement with experimental observations on Fig. 7.

According to Eq 41, the slope of this straight line is given by the ratio of the screw length to the pitch. The theoretical values of the maximum mass and reduced throughput in the intermeshing zone can also be calculated using Eqs 18 and 38, considering an average density of 0.5 for the solid.

Experimental measurements of these quantities can be performed on the reduced plots by considering the point at which a deviation from the straight line is observed. However, it is important to notice that large errors can occur in the determination of the maximum mass and throughput on these plots.

Table 2 shows the predicted and observed values for various pitches and barrel temperatures. The experimental parameters are independent of the temperature; this is consistent with the fact that in this

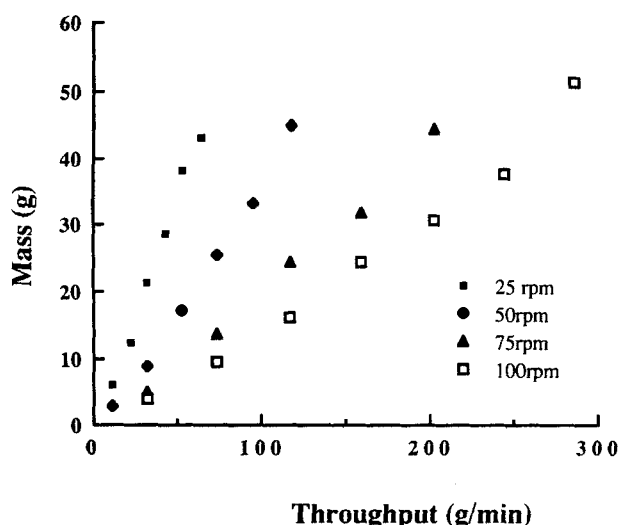


Fig. 6. Mass of material in the screw vs. the mass throughput at various rotational speeds (pitch = 25 mm, barrel temperature = 20°C).

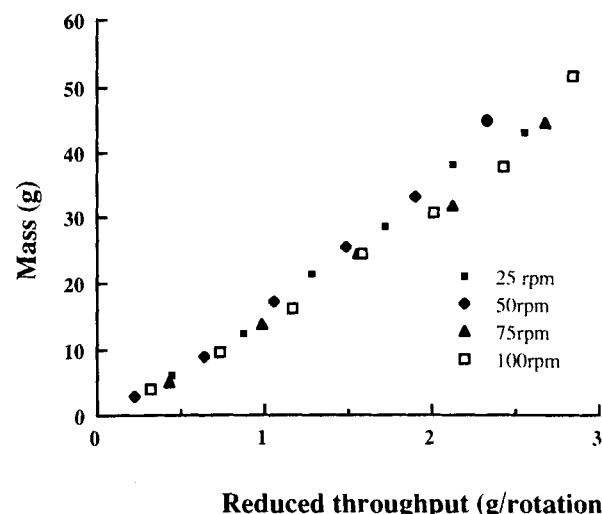


Fig. 7. Mass of material in the screw vs. the reduced mass throughput (pitch = 25 mm, barrel temperature = 20°C).

zone, transport remains independent of the friction coefficients of the solid with the metal.

There is a fair agreement between theoretical and experimental values of the slope of the straight line. However, comparisons for the values of the maxima show relatively poor agreement; this discrepancy is mainly due to the difficulty in measuring these values with high accuracy and in addition to a possible difference in the density of the material in this zone—where a better packing of the powder could be achieved.

### Comparison Between Theory and Experiment in the Channels

For the conveying of the solid material in the channels, according to the model proposed in the present paper, the plot of the mass in the screw vs. the reduced throughput should also yield a straight line. The slope of this line is given by Eq 43. It depends on the angle  $\Phi$ , which is itself a function of the friction coefficients on the screw and on the barrel. At a barrel temperature of 20°C, it is reasonable to assume that these two coefficients are equal. Thus according to Eq 33, calculation of angle  $\Phi$  requires only the knowledge of the ratio  $\frac{x_s}{x_b}$ .

A numerical calculation of  $x_b$  and  $x_s$  was performed after discretization of the channel geometry, as described in Fig. 8. The width of the channel,  $w$ , was divided in  $N_i$  elements whose width is  $\Delta x$  at the barrel diameter; each element was described by its position  $x_j$  and its depth  $h(x_j)$ ; the dimension of contact of this element with the screw is:

$$\Delta x_{sj} = \sqrt{\Delta x^2 + [h(x_j - \Delta x) - h(x_j)]^2} \quad (44)$$

When the width of the channel filled with the solid material is  $x_b$ :

$$x_b = N_b \Delta x \quad \text{with } 0 < N_b < N_i \quad (45)$$

and

$$x_s = \sum_{j=1}^{N_b} \Delta x_{sj} \quad (46)$$

An average value of the ratio  $\frac{x_s}{x_b}$  was evaluated according to Eq 47. A weighting of the influence of  $\frac{x_s}{x_b}$  at a particular filling of the screw was introduced in the averaging to take into account for the relative importance of the filled area.

$$\left( \frac{x_s}{x_b} \right) = \frac{\sum_{N_b=1}^{N_i} \frac{x_s}{x_b} h(x_b)}{\sum_{N_b=1}^{N_i} h(x_b)} \quad (47)$$

Results of the calculation for different pitches can be found in Table 1. In Table 3, the experimental and calculated slopes, maximum mass, and maximum reduced throughputs are indicated, showing a good agreement between the proposed model and the experimental results in various screw geometries.

Values of the experimental slopes at high barrel temperature show the influence of the friction coefficients. At a high temperature of the barrel, the friction coefficient with the barrel can be expected to be

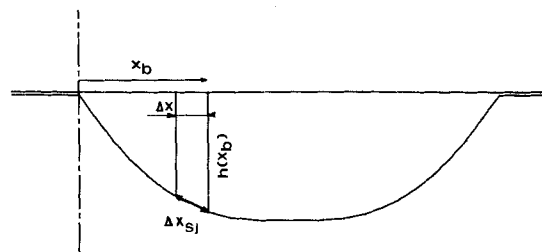


Fig. 8. Discretization of the channel geometry.

Table 2. Characteristic Parameters for the Conveying of Material in the Intermeshing Zone, Predicted and Experimental Values, in Various Conditions.

Pitch (mm)	Experimental Values						Theoretical Values		
	Slope (rot.)		$m_E$ (g)		$Q_E/n$ (g/rot.)		Slope (rot.)	$m_E$ (g)	$Q_E/n$ (g/rot.)
	20°C	100°C	20°C	100°C	20°C	100°C			
16	17.5	17.5	7.3	7.6	0.42	0.43	17.2	6.85	0.40
25	13.0	13.0	8.7	8.7	0.66	0.65	11.0	6.85	0.62
33	10.0	10.0	8.5	8.5	0.85	0.85	8.3	6.85	0.83

Table 3. Characteristic Slopes for the Conveying of Material in the Channels, Maximum Mass, and Maximum Reduced Throughput of the Extruder, Predicted and Experimental Values, in Various Conditions.

Pitch (mm)	Experimental Values						Theoretical Values		
	Slope (rot.)		$M$ (g)		$Q/n$ (g/rot.)		Slope (rot.)	$M$ (g)	$Q/n$ (g/rot.)
	20°C	100°C	20°C	100°C	20°C	100°C			
16	28.6	25.3	41	42	1.6	1.8	30.9	43	1.5
25	20.4	16.5	46	47	2.6	2.9	19.7	43	2.5
33	16.6	14.8	48	45	3.0	3.4	17.1	43	2.9

higher than that of the solid material with the screw. As a consequence, angle  $\Phi$  is increased, leading to significantly lower values of the slope. Unfortunately, we cannot get values of the friction coefficients for the polyethylene powder at this temperature, and these observations remain qualitative.

## DISCUSSION

A comparison between the proposed model and the experimental curves at 20°C is plotted in Fig. 9, and as can be seen, the agreement is good.

Several conclusions can be drawn from the proposed model and the experimental results. First of all, the existence of the intermeshing zone, where material transport takes place whatever the operating conditions are, explains the capability of this type of machine for the extrusion of various materials, even in the case of unfavorable friction coefficients. As can be seen from Tables 2 and 3, the throughput of the intermeshing zone can be evaluated to be about 25% of the maximum throughput of the screws.

Nevertheless, in case of unfavorable friction coefficients, the throughput of the extruder can be limited when the solid fills the channel, because conveying in the channels of the screws is influenced by the friction coefficients. An increase of the friction coefficient of the material with the barrel, by temperature modification for example, enables a more efficient transport of the solid in this zone, leading to an increase in the maximum throughput of the extruder.

In the feeding zone, for a standard screw profile, in which pitches are reduced along the screw, the maximum throughput for solid material in the extruder is that of the zone where the pitch is minimal.

The influence of the operating conditions on the filling of the screws in the feeding zone is described by a single parameter, which is the reduced throughput  $Q/n$ . So an increase of the throughput or a

reduction of the rotational speed can lead to an almost similar filling of the extruder.

In fact, the major interest of this type of modeling is to provide a way to evaluate the filling of the channel in various working conditions. The knowledge of this parameter enables the calculation of the evolution of the solid temperature during its conveying through the feeding zone of the extruder and is a first step in the evaluation of the fusion capacity of the screws for a given profile. The contact area between solid polymer and barrel is a major key to define how thermal transfers occur in this zone. Equations 18 and 37 can be used to evaluate this area.

When the throughput is lower than the maximum throughput of the intermeshing zone,  $Q < Q_E$ , material conveying takes place in the intermeshing area and the contact area between solid and barrel is nearly zero. In these conditions, very little heat transfer is possible.

On the other hand, when  $Q > Q_E$ , transport of material takes place in both the intermeshing zone and the screw channels; the filled area in the channel can then be calculated as:

$$A(x_b) = \frac{(Q - Q_E) \sin \theta_m}{3\pi D n} \frac{tg\Phi + tg\theta}{tg\Phi tg\theta} \quad (48)$$

The evolution of this area vs. the filled width in the channel  $x_b$  can be calculated through:

$$A(x_b) = \int_0^{x_b} h(x) dx \quad (49)$$

and finally the area of contact between the hot barrel and the solid polymer is given by:

$$A_S = 3x_b \frac{L}{\sin \theta} \quad (50)$$

The plot of the contact area  $A_S$  vs. the reduced throughput  $Q/n$  is shown in Fig. 10 for the different screw geometries according to the proposed model. Temperatures of the barrel and screws are taken to be equal, thus defining equal friction coefficients. As can be seen from this plot, in case of small throughput or large rotational speed, the contact area can be nearly zero. In these conditions, the temperature of the solid material will rise slowly and the length of screw needed to reach the molten state can be very large. In standard operating conditions, the zones of small pitches, where the channel is filled, are those where the heating of the solid material takes place. However, in zones where the pitch is so large that conveying takes place mainly in the intermeshing zone, there is no usefulness in imposing a high temperature of the barrel.

## CONCLUSIONS

A theoretical model has been derived for the description of solid conveying in the feeding zone of intermeshing co-rotating twin screw extruders. The model takes into account the particular geometry of the self-wiping twin screw device and the partial fill-

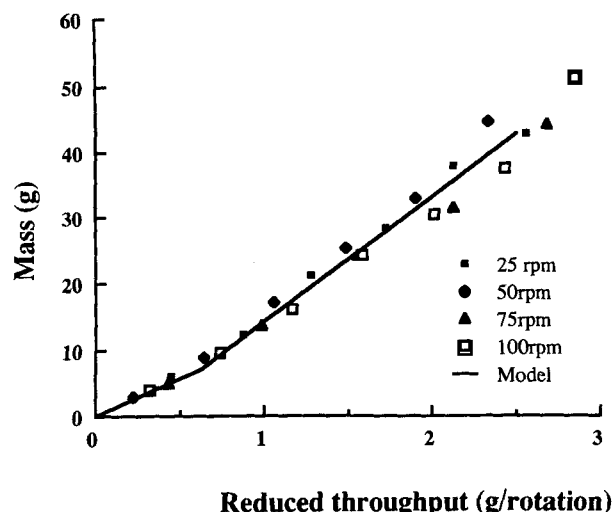


Fig. 9. Comparison between model and experiment. Mass of material in the screw vs. the reduced mass throughput (pitch = 25 mm, barrel temperature = 20°C).



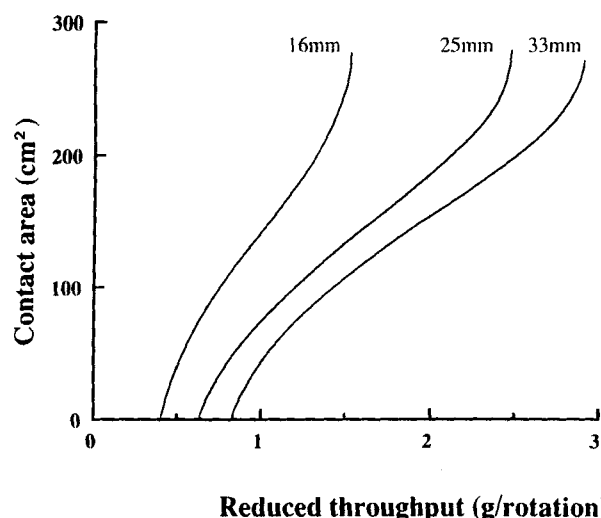


Fig. 10. Contact area between solid material and barrel vs. the reduced throughput for different pitches according to the proposed model (barrel temperature = 20°C).

ing of the channels of the screws. The transport of solid material is investigated in terms of two different mechanisms, which take place either in the intermeshing zone of the screws or in the channels. Theoretical expressions are proposed for these two mechanisms and the global throughput of the extruder was found to be a sum of these two contributions. In the intermeshing zone, material conveying is found to be independent of the friction coefficients, whereas the opposite trend is predicted in the channel.

Experimental verification of the equations was performed by means of a study of the filling of the screw in various operating conditions and various screw geometries. Satisfactory agreement was found between the predictions of the model and the experiments for various screw pitches.

Moreover, this model enables the calculation of the filling of the extruder in various operating conditions. This parameter is an important key for analyzing the evolution of the temperature of the solid material along the screws in the feeding zone. It provides a starting point to define the proper screw profiles to be used to optimize the melting capacity of the extruder.

However, a deeper knowledge of the intermediate zone, where the transition from the solid state to a molten state occurs and where the transported material is a combination of solid and liquid, is now needed to perform a complete description of the working characteristics of this type of machine.

#### NOMENCLATURE

$A_C$	= Channel area.
$A_D$	= screw area.
$A_E$	= Intermeshing zone area.
$A_F$	= Barrel area.
$A_L$	= Free area between barrel and screw.
$A_S$	= Contact area between barrel and solid

material.

$A_U$	= Area of half of a barrel.
$A(x_b)$	= Area of the channel filled with material.
$C_L$	= Centerline distance.
$D$	= Barrel diameter.
$e$	= Flight width.
$f, f_b, f_s$	= Friction coefficients.
$F, F_b, F_s$	= Friction forces.
$h_0$	= Maximum channel depth.
$h$	= Channel depth.
$L$	= Screw length.
$m$	= Number of flight starts.
$M$	= Mass of material in the screw.
$n$	= Rotational speed.
$p$	= Contact pressure.
$Q$	= Total throughput of the extruder.
$Q_C$	= Throughput in the channels.
$Q_E$	= Throughput of the intermeshing zone.
$S$	= Contact area.
$S_E$	= Characteristic slope defined by Eq 41.
$S_C$	= Characteristic slope defined by Eq 43.
$T$	= Pitch.
$u$	= Velocity of a volume element in the channel.
$V_E$	= Material volume in the intermeshing zone.
$V_C$	= Material volume in the channels.
$w$	= Channel width.
$x, x_b, x_s$	= Positions in the channel, normal to the flights.
$z_b, z_s$	= Lengths of the volume elements.
$\alpha$	= Flight angle at the barrel diameter.
$\Phi$	= Angle between the friction force on the barrel and the material velocity.
$\theta, \theta_m, \theta_s$	= Screw angles.
$\rho_c$	= Defined in Eq 2.
$\Psi$	= Angle of the intermeshing zone.

#### REFERENCES

1. C. D. Denson and B. K. Hwang, Jr. *Polym. Eng. Sci.*, **20**, 965 (1980).
2. H. Werner and K. Eise, *SPE ANTEC Tech. Papers*, **25**, 181 (1979).
3. R. A. Lei-fook, A. Senouci, and A. C. Smith, *Polym. Eng. Sci.*, **29**, 433 (1989).
4. J. L. White, *Twin Screw Extrusion, Technology and Principles*, Hanser Verlag, New York (1991).
5. M. L. Booy, *Polym. Eng. Sci.*, **20**, 1220 (1980).
6. H. E. H. Meijer and P. H.M. Elemans, *Polym. Eng. Sci.*, **28**, 275 (1988).
7. W. Szydlowski, R. Brzoskowski, and J. L. White, *Intern. Polym. Processing*, **1**, 207 (1987).
8. W. Szydlowski and J. L. White, *J. Non Newt. Fluid Mech.*, **28**, 29 (1988).
9. F. Martelli, *Twin Screw Extruders, a Basic Understanding*, Van Nostrand Reinhold Co., New York (1983).
10. M. L. Booy, *Polym. Eng. Sci.*, **18**, 973 (1978).
11. Z. Tadmor and I. Klein, *Engineering Principles of Plasticating Extrusion*, Van Nostrand Reinhold Company, New York (1970).
12. P. Avenas, J. F. Agassant, and J. P. Sergent, *La mise en forme des matières Plastiques*, Technique et Documentation Lavoisier, Paris (1982).